

# Sensory data fusion of pressure mattress and wireless inertial magnetic measurement units

Andraž Rihar · Matjaž Mihelj · Janko Kolar ·  
Jure Pašič · Marko Munih

Received: 26 June 2013 / Accepted: 20 October 2014 / Published online: 4 November 2014  
© International Federation for Medical and Biological Engineering 2014

**Abstract** Head movement of infants is an important parameter for analysing infant motor patterns. Despite its importance, this field has received little sensory-based research in the past years. Therefore, we present a sensory-supported data fusion model for head movement analysis of infants in supine position. The sensory system comprises a pressure mattress and two wireless inertial magnetic measurement units, rendering precise, objective and non-intrusive information on pressure distribution and 3D trunk orientation, respectively. Algorithms first perform pressure data pre-processing and calculate image moments to acquire 2D trunk orientation. Afterwards, unscented Kalman filter is used for sensory data fusion. After additional data processing, head and trunk coordinates are calculated along with head displacement distance. The sensory system was tested on experimental measurements, performed in eight normally developing infants aged from 1 to 5 months. Results of several algorithm combinations were compared to referential video recordings in terms of head lifts. Combination of algorithms, incorporating head tracking and sensory data fusion provides completely accurate results in comparison to normative data. Statistical data analysis and referential optoelectronic measurements were performed to evaluate accuracy of the sensory fusion model. Suitability of the proposed sensory system for head movement analysis of infants in supine position was verified.

**Keywords** Sensory data fusion · Pressure mattress · Wireless inertial magnetic measurement units · Infant head movement analysis

## 1 Introduction

Throughout infancy and early childhood, infants gradually develop their motor patterns and progress to higher stages of cognitive development. Insight into infant developmental patterns is very important from a therapist's and parent's point of view, as it can indicate normal or atypical development. The latter can be the result of developmental disorders, especially cerebral palsy (CP) and autism spectrum disorder (ASD), which usually develop throughout infancy and childhood [32]. Infants and children around the globe are affected, with prevalence values that range up to 116/10,000 for ASD [14] and up to 2.5/1,000 for CP [22, 23]. The risk is even higher for very low birth weight infants [29].

Developmental disorders usually result in developmental delays and affect infant posture, motor patterns and cognitive development [32]. Asymmetrical posture, lack of stability or rotation ability [34], hypotonia, unusual posturing [2], along with signs of activity of tonic reflexes, especially spasticity of legs and arms [5, 16], and abnormal arm and finger movement [12], are reported as possible indicators of atypical development. General movements [13, 18] represent another distinct movement parameter, typically studied through video recordings [12, 17, 39] and computer-based video analysis [1, 33]. Parameters like head movement, asymmetrical head posture [5] and active head lifting [19, 38] are also reported as possible indicative measures of CP and cognitive outcome.

Early identification and diagnosis [27] of developmental disorders as well as early intervention [4] are important for

A. Rihar (✉) · M. Mihelj · J. Kolar · J. Pašič · M. Munih  
Laboratory of Robotics, Faculty of Electrical Engineering,  
University of Ljubljana, Ljubljana, Slovenia  
e-mail: andraz.rihar@robo.fe.uni-lj.si  
URL: <http://www.robolab.si>

quality rehabilitation. Researchers are therefore reviewing [27, 40] indicative parameters and preparing questionnaires [30], tests [6, 7] and evaluations [9] in order to increase the percentage of correct diagnoses. Acquisition of posture and movement data is usually supported by various sensory systems, such as video cameras [34], passive marker-based optical systems [26], inertial magnetic systems [35], accelerometers [20], force platforms [24] and pressure mattresses [10, 11].

Even though head movement is clearly as important as trunk posture and other aforementioned parameters, the field of sensory-based head movement research has received little attention over the past years. Rönnqvist et al. [31] studied head position preference of infants using a custom-built platform, focusing on head orientation around one axis. Lee et al. [25] focused on advances in head control due to intensive postural training through a system that provided information on three dimensional head position. Franchak et al. [15] analysed the gaze of older infants by developing a head-mounted eye tracking device. Despite the high precision of the Vicon system [25] and video cameras, all the listed experiments suffer from disadvantages such as invasiveness of the measurement systems (marker arrays, belts, holders and impracticality of head-mounted systems), self-occlusion problems of optical markers [26] and the need for laboratory-based settings [31] with complex and expensive components.

The main goal of this paper is to present a novel sensory system-based computer model for accurate, objective and non-invasive head movement analysis of infants in supine position. Non-invasive assessment of infant head movement is of paramount importance for observing child responses linked to child development. First, the sensory system comprising a pressure mattress and two wireless inertial magnetic measurement units (IMUs) is described. The system is proposed to overcome the aforementioned disadvantages and address the lack of research in the field of head movement. Afterwards, data processing and sensory fusion methods used for infant trunk posture estimation and head position assessment are described. Statistical data analysis and referential measurements are performed to evaluate the accuracy of the proposed sensory system for head movement assessment in terms of head lifts and medial–lateral movement.

## 2 Methods

This section is organised as follows. First, hardware of the experimental set-up and the measurement procedure are presented. Afterwards, the implemented methods and algorithms are described. Finally, a description of the system validation procedure is given.

### 2.1 Hardware

#### 2.1.1 Pressure mattress

A pressure mattress (CONFORMat<sup>®</sup> System, Model 5330, Tekscan, Inc., USA) was used for pressure distribution measurements. The mattress has a total of 1,024 piezoresistive pressure sensors ( $32 \times 32$ ) and dimensions of  $47.1 \text{ cm} \times 47.1 \text{ cm}$ , resulting in an approximate resolution of 0.5 sensors per  $\text{cm}^2$ . Sensors are 0.8 mm thick, while the pressure range of each sensor is 34 kPa.

#### 2.1.2 IMU

Orientation of the infant relative to the mat was acquired using two wireless IMUs, custom built by our research group and thoroughly described in [3]. Each IMU comprises a three-axis gyroscope (InvenSense, Inc., USA), a three-axis accelerometer (STMicroelectronics, Switzerland) and a three-axis magnetometer (Honeywell, USA). The gyroscope has a full-scale range of  $\pm 500^\circ/\text{s}$  and 16-bit resolution, the accelerometer  $\pm 2 \text{ g}$  and 16-bit resolution and the magnetometer has a full-scale range of  $\pm 1.4 \text{ G}$  and 12-bit resolution. Such an assembly provides precise information on angular velocities, acceleration and magnetic field in the local sensor coordinate system. IMU orientation is determined using an unscented Kalman filter, which is described in further detail in the section Software.

#### 2.1.3 Video cameras

Four digital USB video cameras (Webcam C210, Logitech, USA) with resolution  $320 \text{ pixels} \times 240 \text{ pixels}$ , view angle  $53^\circ$  and sampling rate of 10 Hz were used for referential recording of measurement sessions.

### 2.2 Measurement procedure

#### 2.2.1 Subjects

Eight infants aged from 1 to 5 months participated in the study. All the infants were developing normally and were healthy. They were recruited from a private paediatrician clinic at San Piero a Grado (Pisa, Italy). The measurement sessions were approved and overseen by the therapists from IRCCS Fondazione Stella Maris, while the proper informed consent was also obtained from the parents. At least one of them was present throughout the measurement session.

#### 2.2.2 Experimental set-up

Infants were placed on the pressure mattress in supine position, as it is presented with a doll in Fig. 1. The first IMU

was placed near the pressure mattress with a matching orientation and served as a referential sensor (see Fig. 1). During the measurement sessions, this sensor was not moved. The second IMU was put inside a specially designed bracelet that was placed around the infant's chest (see Fig. 1). Digital video cameras were placed above each corner of the experimental set-up to capture the majority of the infants' movements and actions, thus providing reference information for post-session data reviewing. Small speakers and various colour LED lights were set on both sides of the pressure mattress and turned on in a predefined sequence to encourage infant movement and activity. White sheets were hung around the experimental set-up to prevent external disturbances such as infant–mother eye contact.

### 2.2.3 Measurement protocol

In total, approximately 40 min of measurement data were acquired, with each infant's measurement duration being approximately 3–7 min depending on infant's cooperation. Data were acquired simultaneously, with 10 Hz sampling rate for the pressure mattress and 100 Hz sampling rate for the IMUs, and were synchronously processed online using a computer model. Raw sensor data and all the corresponding time stamps were stored on a personal computer hard drive for additional synchronised post-processing offline.

## 2.3 Software

### 2.3.1 Design of the computer model

The computer model is designed and implemented in the mathematical computer programs MATLAB®—Release

2011b, version 7.13 and Simulink—Release 2011b, version 7.8 (The MathWorks, Inc., USA). Sensory data inputs to the computer model are three-dimensional: angular velocity, acceleration, and magnetic field vectors, along with a square-shaped 1,024 element pressure matrix ( $32 \times 32$  elements). The pressure matrix is basically a greyscale digital image with values from 0 to 255. Pressure data are usually subject to bias and crosstalk and should therefore be processed with digital image processing techniques, such as noise removal, comparison to thresholds and segmentation. On the other hand, angular velocity, acceleration, and magnetic field vectors can be processed with sensory fusion techniques, such as unscented Kalman filter, to determine the approximate sensor (trunk IMU) orientation. Unfortunately, the trunk IMU can occasionally be displaced (minimally rotated) during a measurement session, which can result in differences among infant trunk orientation and the trunk IMU orientation.

Precise orientation of the infant trunk is relevant for the head movement analysis for two reasons. First, exact trunk orientation is very important in the process of pressure mattress data segmentation, as it helps determine the approximate head–feet orientation. This is important for recognition of the head imprint patch and subsequent determination of head movement and head lifts. These parameters importantly describe the level of infant's activity and could indicate possible developmental delays. Due to the large variability of pressure mattress data, novel reliable and robust head imprint search algorithms are needed. Second, exact trunk orientation determines the trunk midline, which is important for calculation of head displacement and subsequent analysis of possible asymmetries in the head–trunk posture. To avoid the shortcomings of the inaccurate trunk IMU orientation, use of the image processing techniques (image moments calculation) on the pressure mattress data and subsequent combined use of the pressure and IMU data are proposed as a solution to the given problem. Image moments are basically a weighted average of the image pixel intensities and can be used to describe centroid, area, orientation and other parameters of image patches. In our application, calculation of image moments on an isolated trunk imprint patch could provide additional information on the trunk orientation and determine the trunk midline.

The proposed processing procedure comprises several consecutive modules (see Fig. 2) as follows. First, pressure image moments calculation is performed to determine the two-dimensional trunk orientation ( $\Phi$ ) on the pressure mattress. The calculated orientation and IMU data are further processed in an unscented Kalman filter to improve the accuracy and thus calculate the exact three-dimensional trunk orientation. The image processing module performs detailed pressure imprint data analysis, combining the



**Fig. 1** Experimental set-up, where the doll is equipped with the trunk IMU and placed in supine on the pressure mattress, while the referential IMU is placed in parallel with the pressure mattress

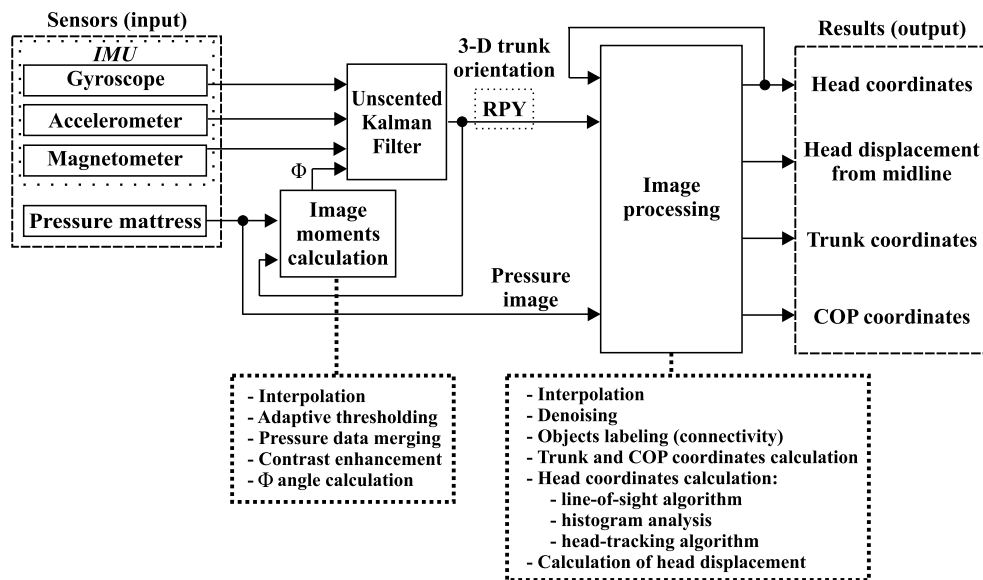


**Fig. 2** Block diagram of the computer model, where RPY represents roll-pitch-yaw (RPY) angles of the three-dimensional trunk orientation, COP depicts COP coordinates of the pressure image and angle  $\Phi$  denotes the two-dimensional trunk orientation on the pressure mattress

original pressure image and the trunk orientation. Finally, head and trunk coordinates, along with head displacement from the trunk midline, are determined as computer model outputs using the image processing techniques.

### 2.3.2 Image moments calculation

Calculation of image moments represents the first module of the computer model (see Fig. 2) and is needed for improving the accuracy of the three-dimensional trunk orientation. It represents the core of the presented methodology and is important especially in cases of unexpected trunk IMU displacement, when IMU is no longer aligned with the infant's longitudinal axis. Image moments calculation module comprises several consecutive steps (see lower left part of Fig. 2). Pre-processing of pressure data using the triangle-based linear interpolation is first applied to increase the quality and resolution of the pressure image (built-in MATLAB library function *griddata*). Afterwards, the two-dimensional eight-connected connectivity method (*bwconncomp*) is used for grouping pressure data into imprint patches. Properties of image regions, such as centroids, areas and loads, are extracted with the imprint patch analysis (*regionprops*). Imprint patch properties are compared to the preset area (10 pixels) and load thresholds to determine the insufficiently loaded imprints. Pixel load threshold is approximately 10 % of the output sensor range and is determined as the bias values of the unloaded pressure mattress data.

Imprint patches in the proximity of the calculated centre-of-pressure (COP) coordinates are combined into the

largest and heaviest imprint patch and thus recognised as the trunk imprint. Proximity area dimensions are adapted with regard to the approximate three-dimensional trunk IMU orientation. At this point, data processing continues by increasing contrast of the trunk pressure data to sufficiently emphasise the trunk imprint orientation. Pressure data corresponding to infant's trunk imprint, already pre-processed, are further used for calculation of raw  $M$  and central  $\mu$  image moments of order up to two. A discrete version of the Eq. (1) is used instead of the original ones published by [21].

$$M_{pq} = \sum_x \sum_y x^p y^q I(x, y)$$

$$\mu_{pq} = \sum_x \sum_y (x - \bar{x})^p (y - \bar{y})^q I(x, y) \quad (1)$$

In (1),  $I(x, y)$  represents the greyscale image pixel intensities,  $x$  and  $y$  are the column and row indices and  $p$  and  $q$  are the moment orders.

A covariance matrix of the normalised second-order central moments is constructed, whereas its eigenvectors correspond to major and minor axes of the image. Orientation can therefore be calculated by (2) and is valid as long as  $\mu_{11}$  is different from 0. Such an orientation could also be obtained by calculation of the first principal component (PCA) of the data. Angle  $\Phi$  will thus be named "PCA" in the presentation of results.

$$\Phi = \arctan \left( \frac{2\mu_{11}}{\mu_{20} - \mu_{02}} \right) \quad (2)$$

In (2),  $\Phi$  is the angle corresponding to orientation of the major axis of trunk imprint in the image, while  $\mu_{11}$ ,  $\mu_{20}$  and  $\mu_{02}$  are the central moments of order up to two.

Exact determination of the trunk imprint is sometimes impossible. In case an infant arches its back, only head, feet or arm imprints are detectable in the pressure data. Insufficient trunk imprint load in comparison to the preset load threshold results in an inability to calculate the image moments. In other cases, when an infant simultaneously raises its head and feet, the trunk imprint is short and circularly shaped. Distinct shape and insufficient major axis length of the trunk imprint (shorter than 40 pixels) again result in an inaccurate trunk orientation. Therefore, the pressure data-based orientation is not forwarded to the UKF in these cases. To retain functionality of the system, the IMU sensory data and the last accurately determined IMU displacement are used as an approximation for orientation calculation and further processing.

### 2.3.3 Unscented Kalman filter

The UKF is an algorithm for estimation of non-linear systems and represents an upgrade to the more frequently used extended Kalman filter (EKF). Along with a few additional calculations, it represents the second module of our computer model (see Fig. 2). A detailed presentation, comparison and description of the UKF and EKF are available in [8, 36, 37]. UKF incorporates the unscented transformation to approximate a Gaussian distribution of a non-linear function. This is done by determining a carefully chosen set of sigma-points to capture the mean and covariance of the random variable. The core of our UKF can be divided into initialisation, time update and measurement update. The last two are also referred to as prediction and correction steps [36]. Throughout the UKF, quaternions are used for orientation description.

The initialisation phase is performed, while the IMUs are in standstill. First, gyroscope biases are calculated as the median values of a 1-s long interval for gyroscope output data. Second, angular velocity, acceleration and magnetic field vectors are normalised by dividing the values with the vector norm and recalculating the data to SI units. Finally, initial orientation of the IMU relative to the Earth coordinate system is determined by calculating the cross product of acceleration and magnetic field vectors. An additional cross product of the acceleration vector and the aforementioned cross product result define the third axis of the coordinate system, consequently fully defining the IMU orientation. Process noise, observation noise and initial state covariance matrices are calculated for further use in time and measurement-update equations. This is followed by determination and propagation of sigma-points through process and measurement models.

The process model relates the current state to the state at a previous time sample. Therefore, during the prediction step, the quaternion is updated by integrating gyroscope data. In other words, current state and covariance are projected ahead and forwarded to the measurement model.

In the measurement model, the predicted current state is corrected in relation to the measurements of accelerometer and magnetometer. By computing the Kalman gain, state and covariance values are updated and corrected quaternion is determined. This quaternion represents rotation from the IMU to the Earth coordinate system.

By quaternion multiplication, rotation from the trunk IMU to the referential IMU coordinate system is acquired. This is followed by transformation of quaternions to roll-pitch-yaw (RPY) angles, representing rotation around the infant's cranial-caudal, medial-lateral and ventral-dorsal axes, respectively.

Whenever pressure data are suitable for orientation determination, the range of  $\Phi$  angle is adjusted and both angles (yaw and  $\Phi$ ) are compared. When necessary, the difference between yaw and  $\Phi$  is calculated, and the estimated trunk IMU quaternion is correspondingly updated around its ventral-dorsal axes. RPY angles are recalculated and provide the image processing module with the 3D trunk orientation description.

### 2.3.4 Image processing

Image processing is the third module of the computer model and serves for detailed infant imprint data analysis (see Fig. 2). Inputs into the module are as follows: pressure matrix, accurate three-dimensional trunk orientation (RPY angles) and head coordinates of the previous time frame (see the head-tracking algorithm description for more details).

The pressure image is first rotated in order to align the trunk orientation (head up) with the orientation of the pressure mattress. This is done to simplify later calculation of coordinates relative to the trunk orientation. Afterwards, the pressure matrix is interpolated using the triangle-based linear interpolation method. Very small artefacts, presumably deriving from small crosstalk of the pressure mattress, are filtered from the image with a specially designed noise removal algorithm as follows. The algorithm first calculates the differences between the minimum and the maximum pixel load values for each imprint patch. All image regions with difference values lower than 5 % of the sensor output range are considered as crosstalk and consequently removed. COP coordinates of the entire image are calculated.

Pressure data are labelled and grouped into imprint patches through search for the connected components (*bwconncomp*), while the imprint data analysis

(*regionprops*) is implemented for determination of patch properties, such as area, load and position.

Patches in the proximity of COP are grouped and identified as the trunk imprint, being the largest and heaviest patch. Trunk coordinates are determined as this patch COP (see Section Image moments calculation for more details on the trunk imprint recognition procedure).

Hereafter, the computer model proceeds with the head imprint search and the head coordinates calculation. This is performed with three head search algorithms as follows. Firstly, the *line-of-sight algorithm* is applied, selecting appropriate patches in the proximity of the approximate shoulder positions. Whenever the head is found successfully, the *head-tracking algorithm* is applied for processing of the following frames, until the head is lifted (the imprint disappears) or the trunk and the head imprints connect (sufficient trunk imprint length). The first option resets the head tracking, and the head search proceeds with the line-of-sight algorithm. In the second case, use of head tracking would eventually result in drift towards the trunk COP due to connection of imprints. Therefore, head tracking is now omitted and the head imprint search is performed with the *histogram analysis*. In case trunk and head imprints are separated again, the head search returns to the line-of-sight algorithm.

**2.3.4.1 Line-of-sight algorithm** The line-of-sight algorithm firstly identifies the approximate chest position of the infant's imprint. This point is determined with respect to known COP coordinates, trunk longitudinal axis orientation and an approximate distance from infant's abdomen to shoulders. Afterwards, the algorithm searches for all the patches within the area, determined as 50° left and right of the trunk orientation direction. Head imprint is recognised as the most loaded imprint patch and its coordinates are calculated. Additionally, the area of the selected imprint patch must be smaller than 500 pixels and the distance of the corresponding centroid to the shoulder position must be lower than 30 pixels. Imprint patches with very small area and load values are removed from the selection. This is implemented in view of avoiding head imprint misidentification.

**2.3.4.2 Head-tracking algorithm** The head-tracking algorithm is based on the premise that head movements have limited dynamics. In case the head is recognised using the line-of-sight algorithm, head tracking is activated and the head coordinates are rerouted to the computer model for processing of the next frame (see Fig. 2). As part of the next frame processing, an area of sufficient dimensions is set around the last determined head coordinates and COP of the imprint inside the area is calculated. Since the head imprint has limited dynamics, these coordinates directly determine the head position in the current time frame. If the head

imprint disappears, while the head and trunk imprints are not connected, both head coordinates are set to zero, indicating a head lift. In case both imprints connect, the head tracking is switched off and the head search proceeds with the histogram analysis.

**2.3.4.3 Histogram analysis** In case the trunk imprint is longer than a preset buttocks to shoulders distance threshold (adapted with respect to the roll angle) and the head patch was not found with the line-of-sight algorithm, this indicates connected imprints of the head and the trunk. This usually occurs when an infant is dressed in a baby dress with a hoodie or when an infant starts slowly lifting its head. In such cases, vertical histogram of the pressure image is calculated. Position of the first peak in the vertical direction (cranial–caudal axes) is extracted to determine the vertical head coordinate. Another horizontal histogram is calculated in the neighbourhood of the vertical head coordinate, whereas its peak determines the horizontal head coordinate.

After determination of the absolute head and trunk coordinates, the distance of head displacement perpendicular to trunk midline is calculated. Since the pressure image is still aligned to the vertical axis, head displacement is a mere deduction of horizontal head and trunk coordinates. Negative and positive values thus indicate head displacement towards right and left side, respectively. Finally, the pressure image and the calculated coordinates are rotated back to the original orientation, the pressure image is displayed, head and trunk coordinates are labelled and the trunk orientation is indicated (see Fig. 3). Head displacement distance (see Fig. 3) and all the calculated coordinates are stored along with the corresponding time stamps for post-processing.

### 2.3.5 Data analysis

The acquired data were additionally post-processed offline with MATLAB® software and built-in functions (*given in parentheses*). Connectivity algorithm (built-in function *bwconncomp*) was applied on one of the head coordinates to group non-zero and zero data into signal segments and determine the total number of head lifts and their duration. Video recordings were carefully reviewed to acquire the number of actual head lifts performed. Head displacement data were analysed by calculating maximum left and maximum right displacements that represent the range-of-motion limits. Median (*median*), mean (*mean*) and standard deviation (SD, *std*) values were extracted to analyse the data for asymmetry. Kurtosis (*kurtosis*) and skewness (*skewness*) parameters were calculated with (3) and (4), as they additionally describe deviance from the Gaussian distribution. Kurtosis indicates how outlier-prone a distribution is, while skewness is a measure of data asymmetry

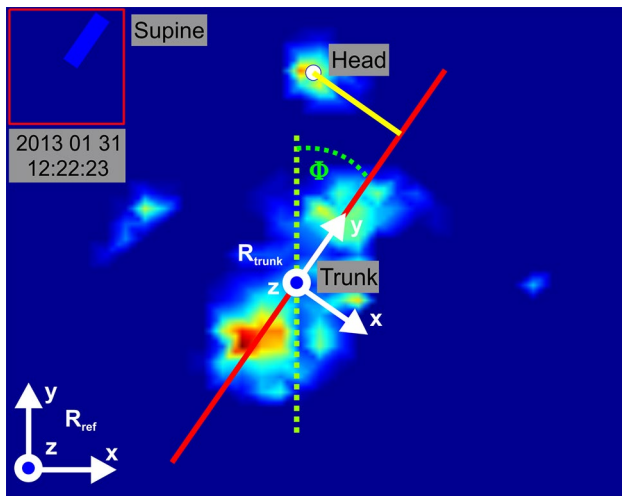


**Fig. 3** Interpolated pressure matrix data with indicated trunk orientation (red line), head displacement distance (yellow line) and angle  $\Phi$  (green lines). Referential IMU coordinate system  $R_{ref}$  is shown in the lower left corner,  $R_{trunk}$  denotes the trunk coordinate system and trunk and head coordinates are labelled with black text (colour figure online)

around the sample mean. Kurtosis and skewness values of a normal distribution are 3 and 0, respectively. Kurtosis values for more and less outlier-prone distributions have values either greater or smaller than 3. Skewness values are either positive for data values spread out to the right or negative for data values spread out to the left.

$$k = \frac{E(x - \mu)^4}{\sigma^4} = \frac{\frac{1}{n} \sum_{i=1}^n (x_i - \bar{x})^4}{\left(\frac{1}{n} \sum_{i=1}^n (x_i - \bar{x})^2\right)^2} \tag{3}$$

$$s = \frac{E(x - \mu)^3}{\sigma^3} = \frac{\frac{1}{n} \sum_{i=1}^n (x_i - \bar{x})^3}{\left(\sqrt{\frac{1}{n} \sum_{i=1}^n (x_i - \bar{x})^2}\right)^3} \tag{4}$$

In (3) and (4),  $\mu$  and  $\bar{x}$  represent mean value of the input data vector  $x$ ,  $\sigma$  is the standard deviation,  $E(t)$  represents expected value of the quantity  $t$  and  $n$  represents quantity of the input data  $x$ .

Root-mean-square (rms) displacement and approximate entropy were calculated to describe the variability and complexity of head displacement time series. Both parameters were already used and verified in infant COP movement analysis and diagnosis of CP [11, 24] and therefore seem potentially useful for illustrating the signal character. A detailed explanation and discussion on approximate entropy can be found in [28]. To acquire a value indicating head activity, travelled distance  $l$  was calculated by (5),

where  $l$  is the travelled distance,  $n$  is the last frame of measurement session and  $x$  and  $y$  are the horizontal and vertical head coordinates, respectively.

$$l = \sum_{i=2}^n \sqrt{(x_i - x_{i-1})^2 + (y_i - y_{i-1})^2} \tag{5}$$

Head movement rate was calculated by dividing the travelled distance  $l$  by duration of the measurement session.

### 2.4 System validation

Referential optoelectronic measurement system OptoTrak Certus (Northern Digital Inc., Waterloo, ON, Canada), providing position accuracy of 0.1 mm at the sampling rate of 100 Hz, was used to validate the proposed measurement system (pressure mattress and two IMUs) for accuracy and reliability. A dedicated baby doll (see Fig. 1) with realistic anthropometric characteristics (weight, height and segment lengths) was used as a test subject, being equipped with one IMU on the trunk and three infrared emitting diodes as active markers on the face (one on the forehead and one on each cheek). Test subject was placed on the pressure mattress in supine position and spontaneous head movement was simulated as follows. Head of the baby doll was moved similar to the head movements, extracted by the careful review of the video recordings. Most of the movement was performed in the dominant direction (medial–lateral), considering the calculated head movement range values for the acquired healthy infant measurement data. One IMU was used as reference and was placed in parallel with the pressure mattress (see Fig. 1). Head position was simultaneously calculated from OptoTrak marker position data as the projected approximate head centre-of-mass and sensory fusion of pressure mattress data and IMUs as the head imprint COP coordinates. Comparison for each coordinate was performed and absolute errors of position determination were calculated for both axes. Accuracy of position data and adequacy of the proposed sensory system were statistically analysed by calculation of Pearson correlation coefficients for each axis.

### 3 Results

This section first provides the head movement results for measurement sessions of eight subjects. This is followed by presentation of the validation results obtained by the proposed sensory system and compared to referential OptoTrak data.

Head movement data, acquired by the proposed measurement system, are presented in terms of head lift, head displacement and head movement distance analysis (see

Table 1). According to the analysis of referential video recordings, eight infants generated six head lifts in total. This number is compared to the head lift results, determined by the analysis of pressure mattress and IMU data. In case that only IMU data is used for trunk orientation determination, the total number of detected head lifts exceeds 100 head lifts. With implementation of the sensory fusion algorithm, which combines the IMU and pressure mattress data for trunk orientation determination, the total number of detected head lifts is reduced to around 50. In case that the head tracking algorithm is used in combination with the sensory fusion method, the total number of detected head lifts is 6.

Head displacement data, determined by the optimum combination of algorithms, were analysed statistically for all eight infants (see Table 1). Median head displacement for infant #1 was lowest with a value of  $-9.6$  cm (see Table 1). Data for infant #1 were highly dispersed (in

the range of 20 cm) with the largest range-of-motion (see Fig. 4 and right part of Fig. 5). Head displacement data of infant #4 had small value dispersion (in the range of 10 cm) with a mean value of 0.8 cm. Dispersion of values for the other infants was mostly around 10 cm with median values near the trunk midline in the range of  $-2$  to  $+2$  cm (see Fig. 4).

Head movement is evaluated with the movement distance and movement rate parameters, indicating level of head activity (Table 1). Infant #7 had the smallest head movement rate of 0.6 cm/s, while infant #3 was most active with the head movement rate of 1.8 cm/s.

Head coordinates for infant #5 are provided in relation to time and as a function of one another to demonstrate the typical head movement of infants (see Fig. 6). The goal is to assess the head movement characteristics in order to appropriately simulate head movement of the dedicated baby doll. The movement exhibits dominance in the

**Table 1** Results of statistical data analysis

		<i>Infants</i>								
		<i>1</i>	<i>2</i>	<i>3</i>	<i>4</i>	<i>5</i>	<i>6</i>	<i>7</i>	<i>8</i>	
<b>Session duration</b>	Session duration [s]	240.9	235.9	159.3	323.5	243.7	451.1	313.0	278.1	
	Head lifted [s]	4.1	1.8	0.0	0.0	0.0	0.9	3.0	0.0	
	Head down [s]	236.7	234.1	159.3	323.5	243.7	450.2	310.0	278.1	
<b>Head lifts</b>	NHT	IMU	2	1/*	0	33	1	71/*	22/*	0
		IMU and PCA	33	3	0	1	5	3	1	1
	HT	IMU	1	3	0	2	1	247/*	15/*	0
		IMU and PCA	1	3	0	0	0	1	1	0
	<b>Video (reference)</b>		<b>1</b>	<b>3</b>	<b>0</b>	<b>0</b>	<b>0</b>	<b>1</b>	<b>1</b>	<b>0</b>
	<b>Head displacement</b>	HT, IMU and PCA	Maximum left [cm]	9.0	6.5	5.4	5.5	16.8	11.3	7.3
Maximum right [cm]			-17.1	-7.0	-6.7	-5.1	-7.8	-5.1	-5.9	-0.7
Median [cm]			-9.6	-1.2	-0.7	0.7	0.6	1.5	0.6	1.5
Mean [cm]			-8.2	-1.4	-0.8	0.8	0.9	1.8	0.9	1.8
Standard deviation [cm]			4.9	1.6	1.1	1.4	2.5	2.0	1.2	1.8
Kurtosis			2.6	4.2	12.2	4.9	13.8	5.0	10.1	27.0
Skewness			0.7	-0.1	-1.1	-0.1	2.4	0.3	1.3	4.6
RMS displacement [cm]			9.6	2.2	1.3	1.6	2.7	2.7	1.4	2.6
Approximate entropy			0.3	0.6	0.4	0.4	0.4	0.5	0.4	0.3
<b>Head coordinates</b>	HT, IMU and PCA	Head movement distance / [cm]	201.0	297.4	282.0	343.6	320.3	429.8	194.9	222.7
		Head movement rate [cm/s]	0.8	1.3	1.8	1.1	1.3	1.0	0.6	0.8

NHT indicates analysis without the head-tracking algorithm, HT indicates inclusion of the head-tracking algorithm

\* Indicates that the head patch was found incorrectly and IMU and PCA indicates that the IMU orientation was corrected by the image moments (PCA) orientation data

medial–lateral direction (see Fig. 6). Horizontal ( $x$  axis) and vertical ( $y$  axis) ranges-of-motion are approximately  $\pm 5$  and  $\pm 1$  cm, respectively.

Finally, validation results are presented as comparison of the head coordinates obtained by OptoTrak and the proposed sensory system (see Fig. 7a, b). The graph is scaled according to the pressure mattress dimensions. Horizontal

( $x$  axis) and vertical ( $y$  axis) ranges-of-motion are approximately  $\pm 5$  and  $\pm 2$  cm with few larger excursions (see Fig. 7a, b). Absolute position estimation error and correlation coefficients (see Fig. 7c) illustrate the level of data similarity and statistically describe accuracy and reliability of the proposed measurement system. The median accuracy for the  $x$  and  $y$  axes were 0.75 and 0.25 cm, respectively, with Pearson correlation coefficients of  $R_x = 0.95$  and  $R_y = 0.73$ .

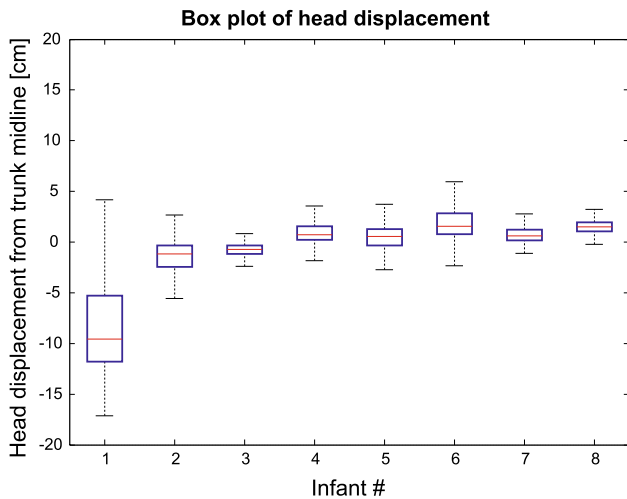
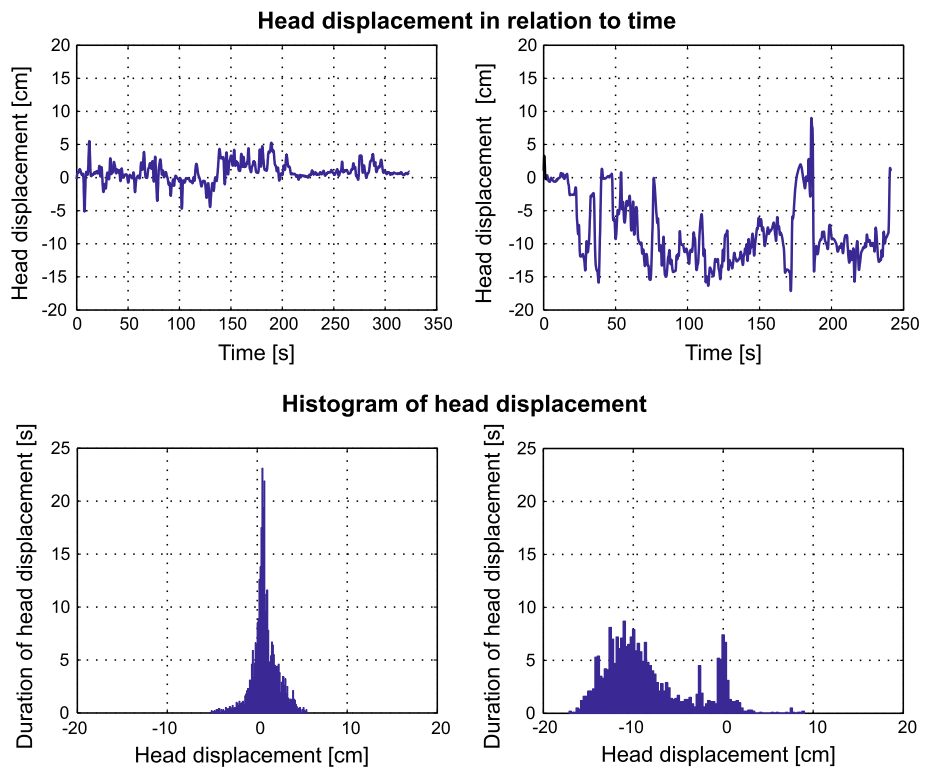


**Fig. 4** Box plot of head displacement data for all eight subjects, indicating median values (red lines), the 25th and 75th data percentiles (blue box edges) and most extreme data points not considered outliers (whiskers). Outliers are not plotted to avoid misinterpretation and incomprehensibility (colour figure online)

**Fig. 5** Time series (upper figures) and corresponding histograms (lower figures) of head displacement for infant #1 (right) and infant #4 (left)



## 4 Discussion

This section first provides a discussion of the implemented head detection algorithms. Following this, comments on the head displacement results are given. Afterwards, the system validation description and acquired accuracy values are presented. Finally, importance of the motor pattern parameters is emphasised and the study limitations are listed.

### 4.1 Head detection algorithms

Various combinations of head detection algorithms (see Table 1) were tested in order to determine the optimal set. Referential review of video recordings was conducted to acquire the number of actual head lifts performed that would make comparison possible.

Results (see Table 1, head lifts section) clearly indicate that head detection, by using only orientation data from

**Fig. 6** Head coordinates in relation to time (*right*) and as a function of one another (*left*) for infant #5

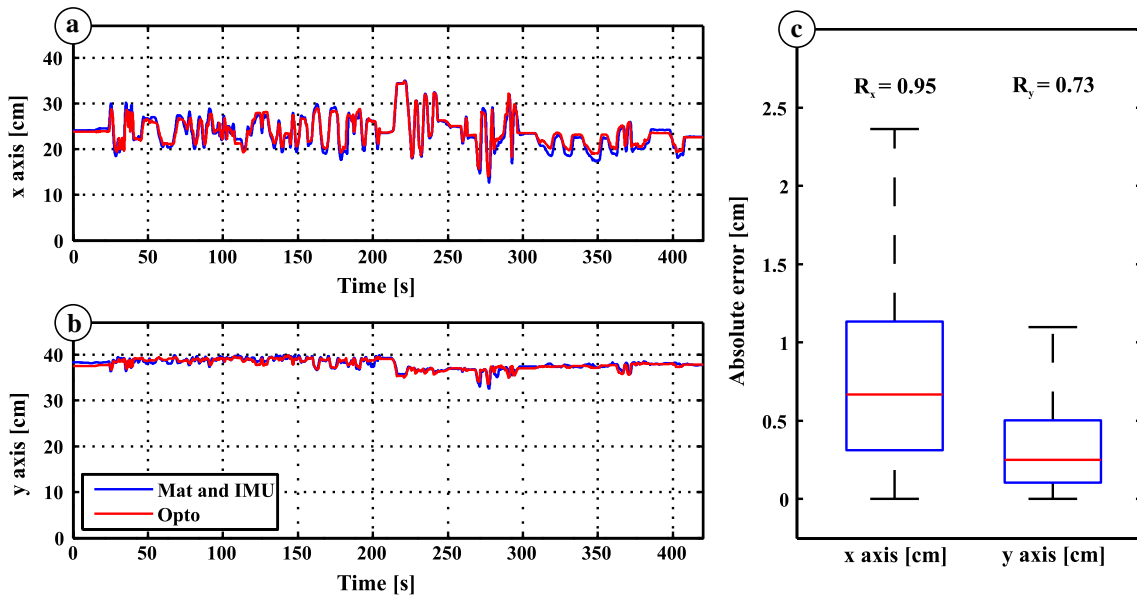
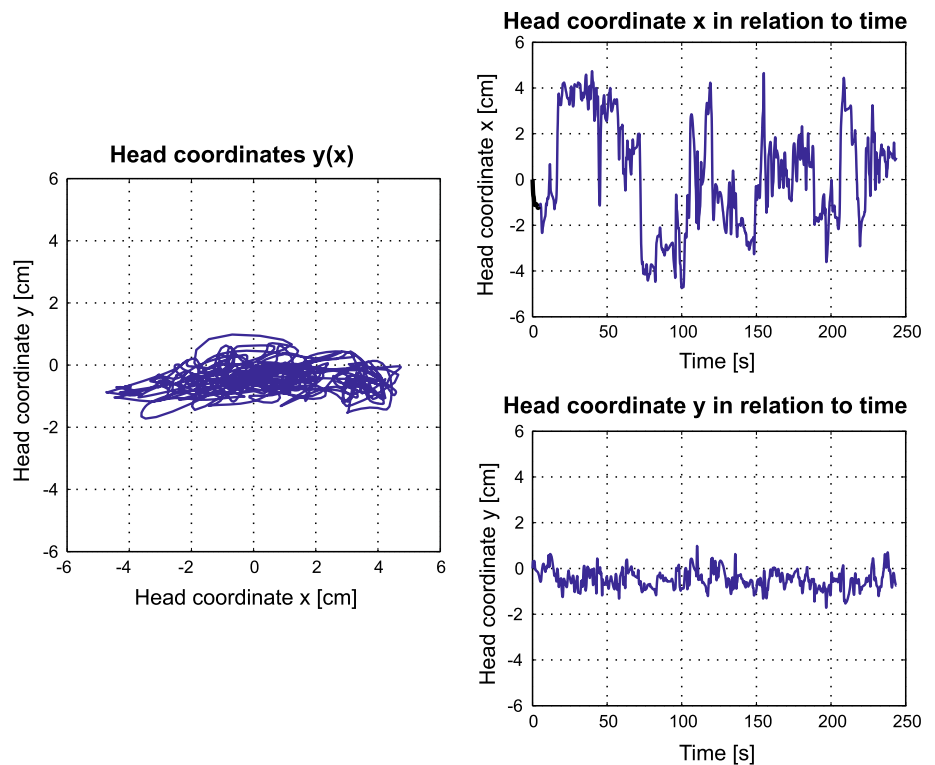


**Fig. 7** Validation results for the head coordinates, where **a** and **b** present the *x* and *y* head coordinates for OptoTrak (*red lines*) and the proposed sensory system (Mat and IMU—*blue lines*), while **c** presents the box plot of absolute errors for both axes. The *red line* represents the median value, *blue box edges* depict the 25th and 75th per-

centiles and the *whiskers* extend to the most extreme data points not considered outliers. Outliers (4.5 % of data for the *x* axis and 2.5 % of data for the *y* axis) are not presented to enhance interpretability of data and ensure clarity of the plot.  $R_x$  and  $R_y$  denote Pearson correlation coefficients for *x* and *y* axes, respectively (colour figure online)

both IMUs, returns incorrect and usually unrealistically high number of head lifts. The high number of head lifts was noted because the infant managed to touch and move

the mounted bracelet while moving its hands during the measurement session. False head detection is also the result of inappropriate fixation of IMUs inside the bracelet, which

resulted in an angle offset in the coronal (frontal) plane. Due to inaccurate angle information, hand imprints were detected and misinterpreted as the head.

These problems were resolved using online adaptive rotation of the IMU quaternion, explained in the section Methods. Incorporation of IMU and pressure mattress sensory data fusion provided correct identification of trunk orientation and consequently successful head imprint detection (see Table 1, IMU and PCA). PCA alone could not be used for determination of head lifts. Since its output angle range is only 180°, preliminary approximate trunk orientation on the pressure mattress must be known and can either be predetermined or measured with an IMU. Another problem emerged when the infant tried to look in either the left or the right direction, consequently rolling its head around the trunk midline axis. This posed another issue for the computer model, as such rotations result in extensive excursions of the head imprint to the opposite direction and simultaneous increase of the head displacement distance. Without the use of the head-tracking algorithm, the line-of-sight algorithm failed to detect the head imprint. This occurred due to the increased head displacement distance and again resulted in false detection of the head imprint and an incorrect number of head lifts.

Head-tracking algorithm therefore provides the computer model with an additionally increased, yet accurate range of detection. Combination of algorithms, incorporating head tracking and sensory data fusion, proved to be completely accurate in comparison with the referential results (see Table 1). Out of almost 40 min of measured data, the computer model managed to correctly detect all six actual head lifts, which confirms its accuracy. Perfect matching of results is not only important in terms of accurate detection of head lifts, but also indicates reliable, correct identification of the head imprint, while the head is in contact with the pressure mattress.

#### 4.2 Head displacement from the trunk midline

The second part of Table 1, Figs. 4 and 5 focus on the head displacement data. Both figures in combination with statistical data provide a good description of data distribution, amplitude and other features of the analysed signal. Negative and positive values of head displacement indicate that infant displaced its head right or left of the trunk midline, which happens when for example an infant rotates its head to look left or right. Maximum left and right values are calculated to identify and measure the full range of the head displacement data. These values can indicate potential limitations of head rotation and movement in relation to the trunk orientation. Median, mean and standard deviation values are calculated to identify asymmetries in the infant's head–trunk posture, which are reported to be important for early diagnosis of autism [34].

Kurtosis is a measure of how outlier-prone a signal distribution is in relation to the normal distribution, while skewness describes asymmetry of data around the signal mean value. Both parameters were thus calculated to provide a good description of the signal distribution, as this can again indicate postural asymmetry. Root mean square displacement and approximate entropy were previously already reported in the analysis of infant's COP patterns [11, 24] and verified as indicators of CP. Analysis of the head coordinates pattern by calculation of approximate entropy is thus also made possible by our computer model.

Statistical values for head displacement are fairly similar for all the measured infants, except for the first one. Video review confirmed that the mentioned infant held its head rotated towards the left throughout most of the session. Visual presentation of data (see Figs. 4, 5) is very useful for easy interpretation and comparison among the measured infants and completely presents the data distribution. Figure 4 indicates that the first infant, while having asymmetrical head posture, has the widest range of head displacement. On the other hand, it indicates that most infants held their head quite still (value dispersion in the range of 10 cm) and mostly near the trunk midline. This is additionally verified by the detailed comparison of the head displacement time series and the histogram data for infant #1 and infant #4 (see Fig. 5). Again, it is evident that the infant #4 held its head near the trunk midline more often, as opposed to the infant #1, which had a wider range of motion and held its head asymmetrically. This verifies that our measurement system and the implemented computer model are capable of detecting and analysing various infant movement activities, including not only still behaviour but also head movements with wide head displacement range.

#### 4.3 Validation of system accuracy

Besides the listed parameters, head coordinates analysis is also provided by the computer model. First, travelled distance of the head coordinates during each session was calculated. These values were also normalised by considering the session duration to indicate the rate of head movement and the infant's activity rate. The visual presentation for the fifth infant (see Fig. 6) again provides easier interpretation of activity in the vertical and the horizontal direction. The latter is more active, which is basically expected. Comparison of such graphs among several infants can demonstrate pattern differences and increased or decreased activity rate.

Accuracy validation results (see Fig. 7) present adequacy of the proposed sensory system for head position recognition and consequent head movement analysis. Comparison to Fig. 6 confirms adequacy of the performed head movements with prevailing movement of larger range in the medial–lateral ( $x$  axis) direction (see Fig. 7a, b). Absolute error

values (median accuracy for the  $x$  and  $y$  axes were 0.75 and 0.25 cm, respectively) reveal high precision of the head coordinates determination. Both Pearson coefficients ( $R_x = 0.95$  and  $R_y = 0.73$ ) indicate high level of determined signal correlation (see Fig. 7c). Higher value for  $x$  axis is expected due to larger range of movement and distinct signal character.

#### 4.4 Importance of the motor pattern parameters

Head movement analysis is especially important during the pre-reaching and the reach-to-grasp development period. Since these motor patterns and developmental milestones are closely related, the typical age group that the system is targeting is 1–7 months, when infants begin to progress towards these developmental milestones.

Finally, it is important to emphasise that although not all of the parameters were compared to the reference measurements, the comprehensive list of parameters is important for thorough, complete description of infant motor patterns. Each of the listed descriptors provides its own insight into the characteristics of infant head movement, focusing either on vertical movement in terms of head lifts or medial–lateral movement in terms of head displacement. Validation of position accuracy by using a referential optoelectronic measurement system is very important, since several parameters (head movement distance and head movement rate) are derived from position data. The numerous parameter results, which are extracted from the pressure mattress and IMU data, indeed ensure non-invasive assessment of infant head movement, which is of major importance for analysis of child development.

#### 4.5 Study limitations

A few limitations of our study should be highlighted: small sample size and relatively young age of infant subjects, small number of tracked head lifts, and a fairly low-sampling rate for the pressure mattress data.

First of all, it should be noted that only eight infants were recruited for our measurement trials. Such a small sample size clearly limits the ability of performing advanced statistical analysis on the acquired data. Such analysis should be performed on a larger pool of data, but this is not the goal of the paper. The main intention of our paper is to present a novel measurement system and sensory fusion method for non-invasive assessment of infant head movement. Therefore, measurement data of eight infants should suffice for presentation of system functionality and the corresponding validation. The recruited infants were aged from 1 to 5 months, thus not covering the full age group range that the system is targeting. Infants from 5 to 7 months of age are usually more active and lift their heads more often. Head movement measurements for this age group could thus represent an important field of research, but taking into

account the scope of our paper, this limitation should not affect our presentation of results.

The second limitation is that the infant subjects in the study generated rather small number of head lifts in total (only 6). This number does seem low for a validation study, as a higher number could additionally support the results. On the other hand, out of almost 40 min of data, our system manages to successfully track all the actual head lifts and correctly determines the head imprint position, while the head is on the pressure mattress. This verifies the correctness and high reliability of our system, implying that a higher number of performed head lifts should not affect the acquired results.

Finally, the sampling rate of 10 Hz for the pressure mattress data does seem relatively low and limits the analysis of movements with extremely short duration. Higher sampling frequency could perhaps provide a more exact description of head movement. On the other hand, infants usually do not perform head movements with duration shorter than 0.1 s; therefore this setting should not affect our study results much.

## 5 Conclusion

Presented results demonstrate correctness of our computer model and therefore verify suitability of the proposed sensory system for head movement analysis of infants in supine position. The proposed system is accurate, reliable, transportable, cost-effective and non-invasive, as proven by the statistical analyses and validation measurements. It avoids several weaknesses of other systems, proposed for similar measurements [25, 31], and exploits several already verified advantages of the proposed sensors [11, 20, 35]. Sensory data fusion increases system reliability and improves accuracy of the used algorithms, as proven by the comparison with referential video recordings.

The proposed sensory system could be of interest to child therapists, paediatricians and other clinical staff, providing a powerful tool for quick, objective and non-invasive infant head movement assessment.

**Acknowledgments** This work was funded by the European Union Collaborative Project CareToy grant ICT-2011.5.1-287932 and additionally supported by the Slovenian Research Agency. The authors gratefully thank Giuseppina Sgandurra, Giovanni Cioni, Francesca Cecchi and Paolo Dario for help with recruitment of infants, experimental set-up and data acquisition.

## References

1. Adde L, Helbostad JL, Jensenius AR, Taraldsen G, Grunewaldt KH, Støen R (2010) Early prediction of cerebral palsy by computer-based video analysis of general movements: a feasibility study. *Dev Med Child Neurol* 52(8):773–778

2. Adrien JL, Lenoir P, Martineau J, Perrot A, Hameruy L, Larmande C, Sauvage D (1993) Blind ratings of early symptoms of autism based upon family home movies. *J Am Acad Child Psychiatry* 32(3):617–626
3. Beravs T, Podobnik J, Munih M (2012) Three-axial accelerometer calibration using Kalman filter covariance matrix for online estimation of optimal sensor orientation. *IEEE Tran Instrum Meas* 61(9):2501–2511
4. Blauw-Hospers CH, Hadders-Algra M (2005) A systematic review of the effects of early intervention on motor development. *Dev Med Child Neurol* 47(6):421–432
5. Bobath K, Bobath B (1956) The diagnosis of cerebral palsy in infancy. *Arch Dis Child* 31(159):408–414
6. Bryson SE, Zwaigenbaum L, McDermott C, Rombough V, Brian J (2008) The autism observation scale for infants: scale development and reliability data. *J Autism Dev Disord* 38(4):731–738
7. Campbell SK, Kolobe TH, Osten ET, Lenke M, Girolami GL (1995) Construct validity of the test of infant motor performance. *Phys Ther* 75(7):585–596
8. Crassidis JL, Markley FL, Cheng Y (2007) Survey of nonlinear attitude estimation methods. *J Guid Control Dyn* 30(1):12–28
9. Darrah J, Piper M, Watt MJ (1998) Assessment of gross motor skills of at-risk infants: predictive validity of the Alberta Infant Motor Scale. *Dev Med Child Neurol* 40(7):485–491
10. Dusing S, Mercer V, Yu B, Reilly M, Thorpe D (2005) Trunk position in supine of infants born preterm and at term: an assessment using a computerised pressure mat. *Pediatr Phys Ther* 17(1):2–10
11. Dusing SC, Kyvelidou A, Mercer VS, Stergiou N (2009) Infants born preterm exhibit different patterns of center-of-pressure movement than infants born at full term. *Phys Ther* 89(12):1354–1362
12. Einspieler C, Cioni G, Paolicelli PB, Bos AF, Dressler A, Ferrari F, Roversi MF, Prechtel HFR (2002) The early markers for later dyskinetic cerebral palsy are different from those for spastic cerebral palsy. *Neuropediatrics* 33(2):73–78
13. Einspieler C, Marschik PB, Bos AF, Ferrari F, Cioni G, Prechtel HFR (2012) Early markers for cerebral palsy: insights from the assessment of general movements. *Future Neurol* 7(6):709–717
14. Elsabbagh M, Divan G, Koh YJ, Kim YS, Kauchali S, Marcini C, Montiel-Nava C, Patel V, Paula CS, Wang C, Yasamy MT, Fombonne E (2012) Global prevalence of autism and other pervasive developmental disorders. *Autism Res* 5(3):160–179
15. Franchak JM, Kretch KS, Soska KC, Adolph KE (2011) Head-mounted eye tracking: a new method to describe infant looking. *Child Dev* 82(6):1738–1750
16. Groot L (2000) Posture and motility in preterm infants. *Dev Med Child Neurol* 42(1):65–68
17. Guzzetta A, Belmonti V, Battini R, Boldrini A, Paolicelli PB, Cioni G (2007) Does the assessment of general movements without video observation reliably predict neurological outcome? *Eur J Paediatr Neurol* 11(6):362–367
18. Hadders-Algra M (2004) General movements: a window for early identification of children at high risk for developmental disorders. *J Pediatr* 145(2):12–18
19. Hadders-Algra M (2012) Active head lifting from supine in infancy: a significant stereotypy? *Dev Med Child Neurol* 54(6):489–490
20. Heinze F, Hesels K, Breitbach-Faller N, Schmitz-Rode T, Diselhorst-Klug C (2010) Movement analysis by accelerometry of newborns and infants for the early detection of movement disorders due to infantile cerebral palsy. *Med Biol Eng Comput* 48(8):765–772
21. Hu MK (1962) Visual pattern recognition by moment invariants. *IRE Tran Inform Theory* 8(2):179–187
22. Johnson A (2002) Prevalence and characteristics of children with cerebral palsy in Europe. *Dev Med Child Neurol* 44(09):633–640
23. Krigger KW (2006) Cerebral palsy: an overview. *Am Fam Physician* 73(1):91–100
24. Kyvelidou A, Harbourne RT, Shostrom VK, Stergiou N (2010) Reliability of center of pressure measures for assessing the development of sitting postural control in infants with or at risk of cerebral palsy. *Arch Phys Med Rehabil* 91(10):1593–1601
25. Lee HM, Galloway JC (2012) Early intensive postural and movement training advances head control in very young infants. *Phys Ther* 92(7):935–947
26. Meinecke L, Breitbach-Faller N, Bartz C, Damen R, Rau G, Diselhorst-Klug C (2006) Movement analysis in the early detection of newborns at risk for developing spasticity due to infantile cerebral palsy. *Hum Mov Sci* 25(2):125–144
27. Palmer FB (2004) Strategies for the early diagnosis of cerebral palsy. *J Pediatr* 145(2):S8–S11
28. Pincus SM, Goldberger AL (1994) Physiological time-series analysis: what does regularity quantify? *Am J Physiol Heart C* 266(4):H1643–H1656
29. Platt MJ, Cans C, Johnson A, Surman G, Topp M, Torrioli MG, Krageloh-Mann I (2007) Trends in cerebral palsy among infants of very low birthweight (<1500 g) or born prematurely (<32 weeks) in 16 European centres: a database study. *Lancet* 369(9555):43–50
30. Robins DL, Fein D, Barton ML, Green JA (2001) The modified checklist for autism in toddlers: an initial study investigating the early detection of autism and pervasive developmental disorders. *J Autism Dev Disord* 31(2):131–144
31. Rönnqvist L, Hopkins B (1998) Head position preference in the human newborn: a new look. *Child Dev* 69(1):13–23
32. Rosenbaum P, Paneth N, Leviton A, Goldstein M, Bax M, Damiano D, Dan B, Jacobsson B (2007) A report: the definition and classification of cerebral palsy April 2006. *Dev Med Child Neurol* 49(Suppl 109):8–14
33. Stahl A, Schellewald C, Stavadahl Ø, Aamo OM, Adde L, Kirkeroed H (2012) An optical flow-based method to predict infantile cerebral palsy. *IEEE Tran Neural Syst Rehabil* 20(4):605–614
34. Teitelbaum P, Teitelbaum O, Nye J, Fryman J, Maurer RG (1998) Movement analysis in infancy may be useful for early diagnosis of autism. *Proc Natl Acad Sci USA* 95(23):13982–13987
35. van den Noort JC, Ferrari A, Cutti AG, Becher JG, Harlaar J (2013) Gait analysis in children with cerebral palsy via inertial and magnetic sensors. *Med Biol Eng Comput* 51(4):1–10
36. van der Merwe R (2004) Sigma-point Kalman filters for probabilistic inference in dynamic state-space models. PhD Thesis, University of Stellenbosch, Western Cape, South Africa
37. VanDyke MC, Schwartz JL, Hall CD (2004) Unscented Kalman filtering for spacecraft attitude state and parameter estimation. Department of Aerospace & Ocean Engineering, Virginia Polytechnic Institute & State University, Blacksburg, Virginia
38. van Haastert IC, Groenendaal F, van de Waarsenburg MK, Eijssermans MJ, Koopman-Esseboom C, Jongmans MJ, Helders PJM, de Vries LS (2012) Active head lifting from supine in early infancy: an indicator for non-optimal cognitive outcome in late infancy. *Dev Med Child Neurol* 54(6):538–543
39. Yuge M, Marschik PB, Nakajima Y, Yamori Y, Kanda T, Hirota H, Yoshida N, Einspieler C (2011) Movements and postures of infants aged 3 to 5 months: to what extent is their optimality related to perinatal events and to the neurological outcome? *Early Hum Dev* 87(3):231–237
40. Zwaigenbaum L, Bryson S, Rogers T, Roberts W, Brian J, Szatmari P (2005) Behavioral manifestations of autism in the first year of life. *Int J Dev Neurosci* 23(2):143–152